Journal of proteome research

Article

pubs.acs.org/jpr

Comparative Proteomic Analysis of the Thermotolerant Plant *Portulaca oleracea* Acclimation to Combined High Temperature and Humidity Stress

Yunqiang Yang,[†,$,‡] Jinhui Chen,[§,‡] Qi Liu,[∥] Cécile Ben,[#] Christopher D. Todd,[⊥] Jisen Shi,[§] Yongping Yang,*[,†] and Xiangyang Hu*[,†]

[†]Key Laboratory of Biodiversity and Biogeography, Kunming Institute of Botany, Institute of Tibet Plateau Research, Chinese Academy of Science, Kunming 650204, China

[$]Graduate University of Chinese Academy of Sciences, Beijing, 100049, China

[§]Key Laboratory of Forest Genetics & Biotechnology, Nanjing Forestry University, Nanjing 210037, China

[∥]Institute of Genomic Medicine, Wenzhou Medical College, Wenzhou 325035, China

[#]Université de Toulouse, EcoLab, Castanet Tolosan, 31326, France

[⊥]Department of Biology, University of Saskatchewan, Saskatoon, Canada S7N 5E2

Supporting Information

ABSTRACT: Elevated temperature and humidity are major environmental factors limiting crop yield and distribution. An understanding of the mechanisms underlying plant tolerance to high temperature and humidity may facilitate the development of cultivars adaptable to warm or humid regions. Under conditions of 90% humidity and 35 °C, the thermotolerant plant *Portulaca oleracea* exhibits excellent photosynthetic capability and relatively little oxidative damage. To determine the proteomic response that occurs in leaves of *P. oleracea* following exposure to high temperature and high humidity, a proteomic approach was performed to identify protein changes. A total of 51 differentially expressed proteins were detected and characterized functionally and structurally; these identified proteins were involved in various functional categories, mainly including material and energy metabolism, the antioxidant defense responses, protein destination and storage, and transcriptional regulation. The subset of antioxidant defense-related proteins demonstrated marked increases in activity with exposure to heat and humidity, which led to lower accumulations of H_2O_2 and O_2^- in *P. oleracea* compared with the thermosensitive plant *Arabidopsis thaliana*. The quickly accumulations of proline content and heat-shock proteins, and depleting abscisic acid (ABA) via increasing ABA-8′-hydroxylase were also found in *P. oleracea* under stress conditions, that resulted into greater stomata conductance and respiration rates. On the basis of these findings, we propose that *P. oleracea* employs multiple strategies to enhance its adaptation to high-temperature and high-humidity conditions.

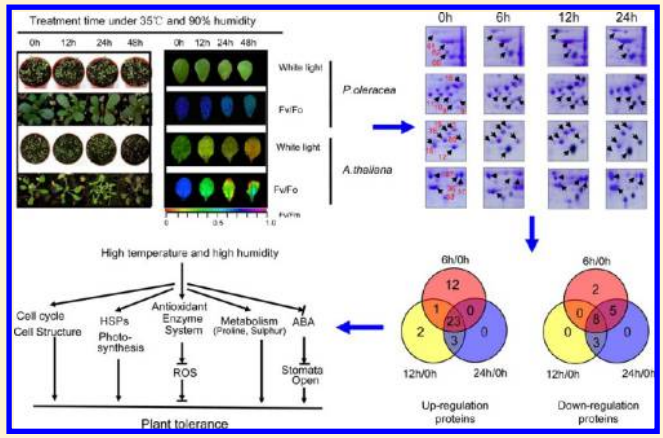

KEYWORDS: *ABA, high temperature, high humidity, Portulaca oleracea, ROS*

INTRODUCTION

High temperature and high humidity typically are characterized as independent abiotic stress conditions. In tropical climates, however, they occur simultaneously and are the primary environmental factors limiting the geographical distribution and productivity of plants. Crop-based modeling and empirical studies in tropical and subtropical regions have reported 2.5−16% direct yield losses of major crops for every 1 °C increase in seasonal temperature.[1] High temperature induces sterility in wheat grain, and high humidity intensifies this response.[2,3] High humidity can exacerbate the damaging effect of high temperature by restricting transpiration (i.e., moisture loss from leaves), which is essential to lowering the surface temperature of leaves and promoting water and mineral uptake and motility.[3] Moreover, high humidity enhances the damaging effects of air pollution (e.g., ozone) and promotes the spread of infection by increasing the stomatal aperture size.[4−6] The photosynthetic apparatus associated with photosystem (PS) II is highly sensitive to heat stress and humidity; these stressors may damage stomatal conductance.[6] Wang et al.[7] reported that high temperature and humidity stress decreased digalactosyl-

Received: January 10, 2012
Published: May 23, 2012

diacylglycerol synthase and magnesium-chelatase while increasing ribulose bisphosphate carboxylase/oxygenase proteins. This association reflects a reduction in photosynthetic rate and an increase in the rate of photorespiration. An understanding of the mechanisms of plant adaptations to heat and humidity stressors could facilitate the development of cultivars with improved productivity in warm, humid climates.

Plant adaptation to adverse milieus is dependent upon the activation of cascades of molecular networks associated with stress perception. Signal transduction and the expression of stress-related proteins protect the essential structures and functions of cells from stress-induced damage. Proteomic analyses provide powerful tools for understanding the protein machinery at the organelle, cell, tissue, or organ levels. Comparative proteomics can shed light on the physiological response to varying, potentially harmful environmental conditions at the whole-plant level. Several studies have examined the heat-stress-induced proteomic responses of monocotyledonous crop plants.[8] Changes in protein expression have been demonstrated during heat stress in several noncrop model plants, including *Populus*, Norway spruce, and *Agrostis*.[9] However, proteomic and functional analyses of plants exposed to multiple, synchronous stresses (e.g., high temperature and humidity) still are needed.

Acclimation to thermal stress in both plants and animals is dependent upon multiple pathways, particularly those involving heat shock proteins (HSPs).[10,11] HSPs can be classified as small HSPs, including HSP15 and HSP28 (with molecular weights 15 and 28 kDa, respectively); moderately sized HSPs, such as HSP60 and HSP70; and large HSPs, including HSP90 and HSP101. Most HSPs protect against protein misfolding and aggregation during heat stress, but each HSP family has a distinct mechanism of action.[12] For example, HSP60 and HSP70 can prevent protein aggregation by binding to protein intermediates,[13] whereas HSP101 can reactivate proteins that have already aggregated.

Environmental stressors also trigger the accumulation of compatible osmolytes, including sucrose, proline, betaine, and polyamine, that contribute to protein stability.[14,15] The synthesis of proline from L-glutamic acid via Δ^1-pyrroline- 5-carboxylate (P5C) is catalyzed in plants by the activities of P5C synthetase (P5CS) and P5C reductase (P5CR).[16,17] Many additional messenger molecules, such as abscisic acid (ABA), salicylic acid, and nitric oxide, also contribute to thermal responses in plants.[18,19] Indeed, plants utilize marked plasticity to adapt to complex environmental conditions.

Prior reports have focused on the plant response to a single abiotic stress at the physiological or transcriptional level.[13−15] These studies do not represent an accurate picture of environmental stress; in nature, plants may be exposed to many abiotic stresses simultaneously. A series of studies investigating plant responses to concomitant stresses are warranted to improve our comprehensive knowledge of the complexity of plant metabolic networks during stress. Such work is expected to aid in the development of novel plant breeding strategies.

In plants, exposure to elevated temperature induces an excessive accumulation of reactive oxygen species (ROS), including hydrogen peroxide and superoxide ions, that seriously damage the cellular membrane and internal functional components.[20] The ascorbate−glutathione cycle plays a key role in scavenging ROS from cells.[21,22] During this cycle, H_2O_2 is degraded by ascorbate peroxidase (APX) using ascorbic acid (ASA) as an electron donor and yielding a short-lived monodehydroascorbate radical that is directly reduced to ASC and dehydroascorbate (DHA). DHA, in turn, is reduced by dehydroascorbate reductase (DHAR) or monodehydroascorbate reductase (MDHAR) using glutathione (GSH) as an electron donor to produce glutathione disulfide (GSSG), the oxidized product. The GSSG is recycled to GSH via NADPH-dependent GSH reductase (GR). In addition, ASA can react directly with hydroxyl radicals, superoxide anions, and singlet oxygen molecules to prevent ROS damage. The ascorbate−glutathione antioxidant system is well characterized in plants under various single environmental stress conditions,[21,22] However, its function during simultaneous temperature and humidity stressors remains unclear.

Some plant species have evolved protective mechanisms to ameliorate damage from adverse environmental conditions. *Portulaca oleracea* is a thermotolerant plant species that is widely distributed in tropical regions and can survive ambient temperatures exceeding 35 °C and 90% relative humidity for several days. We applied physiological and comparative proteomics to investigate the mechanisms underlying *P. oleracea*'s tolerance of high-temperature and high-humidity stress. Our results demonstrate that *P. oleracea* deploys multiple strategies to cope with these combined stressors. By characterizing the adaptive mechanisms of *P. oleracea* to heat and humidity, we may ultimately be able to apply focused breeding strategies to improve crop productivity in warm, humid climates.

MATERIALS AND METHODS

Plant Material and Treatment

P. oleracea and *Arabidopsis thaliana* seeds were germinated and grown in a phytotron under conditions of 25 °C, 65% relative humidity, 300 μmol s^{-1} m^{-2} light intensity, 12-h light/12-h dark cycles, and once daily full irrigation. Mature plants grown for 3 weeks were used in subsequent experiments. Heat/humidity challenges were performed by exposing *P. oleracea* and *A. thaliana* to 35 °C and 90% relative humidity. After different time of exposure, the plants were harvested for immediate analysis.

Physiological Analysis

Chlorophyll fluorescence was analyzed using a pulse-amplitude modulation (PAM) chlorophyll fluorometer (Heinz Walz GmbH, Effeltrich, Germany). To measure the maximum quantum yield of PS II (i.e., the ratio of variable to maximum fluorescence, F_v/F_m), plants were dark-adapted for 30 min after 3 d of exposure to 35 °C and 90% relative humidity. The maximum fluorescence (F_m) was recorded by a 0.8 s pulsed light at 4000 μmol s^{-1} m^{-2}. F_v/F_m was determined for each plant using a whole leaf as the area of interest. The leaf stomatal conductance and transpiration ratio were measured using LI-COR 6400 portable gas analyzer (LI-COR, Lincoln, NE) with a light-emitting diode light source every 24 h during stress treatment. The malondialdehyde (MDA) content was measured as previously described.[23]

Protein Extraction and Two-Dimensional Gel Electrophoresis

Protein extraction and two-dimensional electrophoretic (2DE) separation were performed as previously described, with minor modifications.[24] Briefly, 10−20 g of treated leaves was ground in liquid nitrogen, and total soluble proteins were extracted at 4

dx.doi.org/10.1021/pr300027a | J. Proteome Res. 2012, 11, 3605−3623

°C in 5 mL of 50 mM Tris-HCl buffer (pH 7.5) containing 20 mM KCl, 13 mM dithiothreitol (DTT), 2% (v/v) NP-40, 150 mM phenylmethylsulfonyl fluoride (PMSF), and 1% (w/v) PVP. Homogenates were centrifuged at 12 000*g* for 15 min at 4 °C, and the supernatants were added to 5 vol of acetone containing 10% (w/v) TCA and 1% (w/v) DTT. Samples were maintained at −20 °C for 4 h and then were centrifuged at 25 000*g* for 30 min at 4 °C. The resulting pellets were washed with acetone containing 1% (w/v) DTT at −20 °C for 1 h, and the acetone wash was repeated after centrifugation. The final pellets were vacuum-dried and dissolved in 8 M urea, 20 mM DTT, 4% (w/v) CHAPS, and 2% (w/v) ampholyte (pH 3−10). Samples in ampholyte were vortexed thoroughly for 1 h at room temperature and then were centrifuged at 25 000*g* for 20 min at 20 °C. Supernatants then were collected for 2DE experiments, which were conducted in triplicate. Extracted proteins were first separated by isoelectric focusing (IEF) using gel strips to form an immobilized nonlinear pH gradient from 4 to 7 (Immobiline DryStrip, pH 4−7 NL, 17 cm, Bio-Rad, Hercules, CA). Following IEF, proteins were separated by sodium dodecyl sulfate−polyacrylamide gel electrophoresis (SDS-PAGE) using 12.5% (w/v) polyacrylamide. Gel strips then were rehydrated in 450 μL of dehydration buffer containing 800 μg of total proteins and a trace of bromophenol blue for 16 h. Gel strips were focused at 64 kV/h and 20 °C using the PROTEAN IEF system (Bio-Rad) and then were equilibrated for 15 min in equilibration buffer (6 M urea, 0.375 M Tris [pH 8.8], 2% [w/v] SDS, 20% [v/v] glycerol, 2% [w/v] DTT). Gel strips then were placed over 12.5% (w/v) SDS-PAGE gels for 2DE. Gel electrophoresis was performed at 25 mA for 5 h. Gels were stained using colloidal Coomassie Brilliant Blue (CBB). After staining, gels were scanned using PDQuest 2-D analysis software (Bio-Rad). Parameters were optimized as follows: saliency, 2.0; partial threshold, 4; minimum area, 50. Protein expression levels were quantified by determining the ratio of the volume of a single spot to the volume of the entire set of spots on the gel. Statistical significance was assigned at $p < 0.05$ for the analysis of parallel spots between different treatments using one-way ANOVA. SPSS (Statistical Package for the Social Sciences) software was used for all statistical analyses (http://spss.en.softonic.com/). To compensate for subtle differences in sample loading or gel staining/destaining across individual experiments, the volume of each spot was normalized as previously described.[24]

In-Gel Digestion

Protein spots displaying significant changes in abundance following plant exposure to high heat/humidity were excised manually from colloidal CBB stained 2DE gels using sterile pipet tips. Spots were transferred to 1.5-mL sterile tubes, destained with 50 mM NH_4HCO_3 at 40 °C for 1 h, reduced with 10 mM DTT in 100 mM NH_4HCO_3 at 60 °C for 1 h, and incubated with 40 mM iodoacetamide in 100 mM NH_4HCO_3 for 30 min. Gels then were minced, air-dried, and rehydrated in 12.5 ng/μL sequencing grade modified trypsin (Promega, Madison, WI) and 25 mM NH_4HCO_3 at 37 °C overnight. Tryptic peptides were extracted from the gel grains thrice using 0.1% trifluoroacetic acid (TFA) in 50% acetonitrile. Supernatants were concentrated to approximately 10 μL using a SpeedVac (Savant Instruments, Inc., Hicksville, NY,) and were desalted using reversed-phase ZipTip pipet tips (C18, P10, Millipore, Billerica, MA). Peptides were eluted with 50% acetonitrile and 0.1% TFA. Protein spots that fluctuated by more than 1.5-fold and passed the Student's *t*-test ($p < 0.05$) were selected and subsequently analyzed by mass spectrometry (MS).

MS Analysis and Database Search

Lyophilized peptide samples were dissolved in 0.1% TFA, and MS analysis was conducted using a 4800 Plus Matrix-Assisted Laser Desorption/Ionization-Tandem Time of Flight (MALDI-TOF/TOF) Proteomics Analyzer (Applied Biosystems, Bedford, MA). MS acquisition and processing parameters were set to reflector-positive mode and an 800−3500-Da acquisition mass range, respectively. The laser frequency was 50 Hz, and 700 laser points were collected for each sample signal. For secondary MS analysis, 4−6 ion peaks with signal-to-noise ratios exceeding 100 were selected from each sample as precursors. The TOF/TOF signal for each precursor then was accumulated with 2000 laser pulse. Primary and secondary mass spectra were transferred to Excel files and input in a nonredundant NCBI database (NCBI-nr 20101014) restricted to Viridiplantae (i.e., green plants) using a MASCOT search engine (www.matrixscience.com). The following search parameters were used: no molecular weight restriction, one missed trypsin cleavage allowed, iodoacetamide-treated cysteine, oxidation of methionine, a peptide tolerance of 100 ppm, and an MS/MS tolerance of 0.25 kDa. Protein identifications were validated manually with at least 3 peptides matched, the keratin contamination was removed, and the MOWSE threshold was set over 60 ($p < 0.05$). According to the MASCOT probability analysis, only significant hits were accepted for the identification of a protein sample.

Antioxidant Activity

Approximately 10−20 g of leaves collected from plants treated for indicated time was homogenized in 50 mM sodium phosphate extraction buffer (pH 7.0) containing 1.0 mM ethylenediaminetetraacetic acid, 0.5% (v/v) Triton X-100, and 1% (w/v) polyvinylpyrrolidone (100 mg tissue/mL buffer). For the analysis of APX, the extraction buffer also contained 5 mM ASA. Homogenates were centrifuged at 15 000*g* for 20 min at 4 °C, and the total soluble protein contents in the supernatants were measured using the Bradford method.[25] The activities of APX (EC1.11.1.11), superoxide dismutase (SOD, EC1.15.1.1), and GR (EC1.6.4.2) in the supernatants were determined using the described method.[26,27]

H_2O_2 and O_2^- Detection

H_2O_2 and O_2^- were detected *in situ* as previously described.[26] The exact locations of H_2O_2 in the tissue were determined using a cytochemical method. Cerium perhydroxide ($CeCl_3$)-based transmission electron microscopy (TEM) was used for cytochemical detection of H_2O_2 in roots. The H_2O_2 content was measured by chemical colorimetry. Briefly, treated leaves were snap-frozen in liquid nitrogen and were homogenized in 10 mM Tris-HCl (pH 8.0) supplemented with 1 mM PMSF, 10 mM $MgSO_4$, 5 mM KCl, 5 mM NaCl, and 10 μM oxyhemoglobin. Homogenates were centrifuged at 15 000*g* for 10 min at 4 °C, and supernatants were collected for subsequent analyses. H_2O_2 measurements were conducted as previously described.[28]

ABA and Proline Content

The ABA content was measured as reported previously.[29] In brief, 200 mg of treated fresh leaf samples was quickly frozen, powdered in liquid nitrogen, and shaken in 1 mL of distilled water for 24 h at 4 °C in the dark. Homogenates were

dx.doi.org/10.1021/pr300027a | J. Proteome Res. 2012, 11, 3605−3623

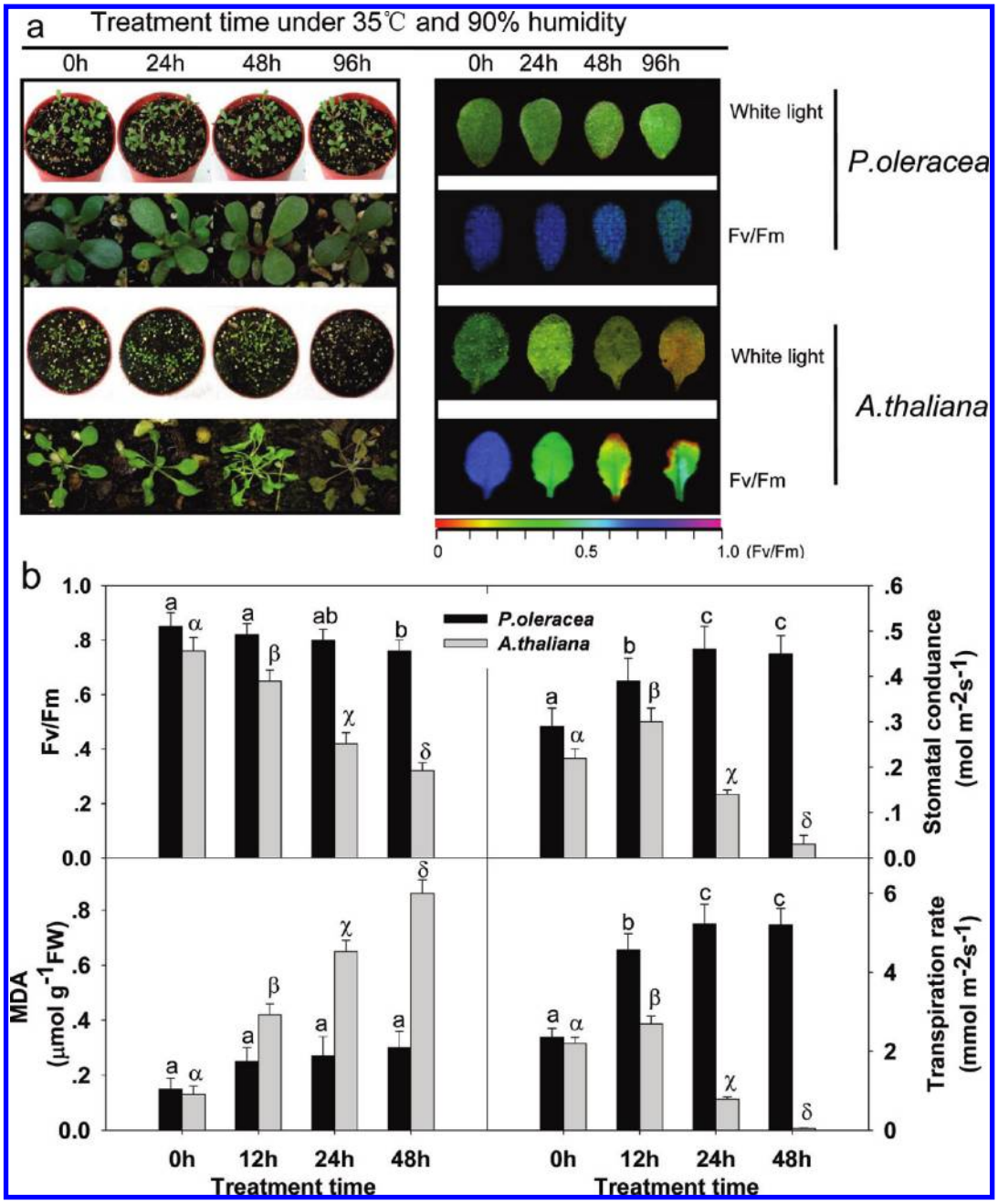

Figure 1. Responses of *P. oleracea* and *A. thaliana* to combined high-temperature and high-humidity stressors. (a) Leaf phenotypes of *P. oleracea* and *A. thaliana* following exposure to high temperature and high humidity. Seedlings were cultivated under normal conditions (25 °C and 65% humidity) for 3 weeks and then were shifted to ambient conditions of 35 °C and 90% relative humidity. At the indicated times, images were captured (left), and photosynthetic capabilities were recorded by F_v/F_m imaging using a PAM chlorophyll fluorometer (right). Images captured under white light were used as controls. The pseudocolor code depicted at the bottom of the images ranges from 0 (red) to 1.0 (purple). (b) The effects of high temperature (35 °C) and high humidity (90%) on photosynthetic F_v/F_m ratio, leaf MDA content, stomatal conductance, and transpiration rate. After 3 weeks of growth under normal conditions, *P. oleracea* and *A. thaliana* seedlings were exposed to conditions of 35 °C and 90% relative humidity. Changes in MDA level, chlorophyll content, stomata conductance, and transpiration rate then were measured at the indicated times. Data are represented as mean values of five replicate experiments (±SE). Mean values indicated by different letters denote significant differences ($p < 0.05$, Tukey's test).

centrifuged at 12 000*g* for 10 min at 4 °C, and supernatants were submitted to the ABA assay. Crude extracts (100 μL) were mixed with 200 μL of phosphate-buffered saline (pH 6.0), 100 μL of ABA antibody (diluted 1:5000, Agrisera, Sweden), and 100 μL of [^{3}H]ABA (~8000 cpm). The reaction mixture was incubated at 4 °C for 45 min, and bound radioactivity was measured in 50% saturated $(NH_4)_2SO_4$-precipitated pellets using a liquid scintillation counter. Proline contents were measured as previously reported.[29,30]

Western Blotting

SDS-PAGE was performed through 12% (w/v) polyacrylamide gels.[31] Protein samples then were electrotransferred onto polyvinylidene difluoride membranes using a Trans-Blot cell (Bio-Rad). Membranes were probed with the appropriate

dx.doi.org/10.1021/pr300027a | J. Proteome Res. 2012, 11, 3605−3623

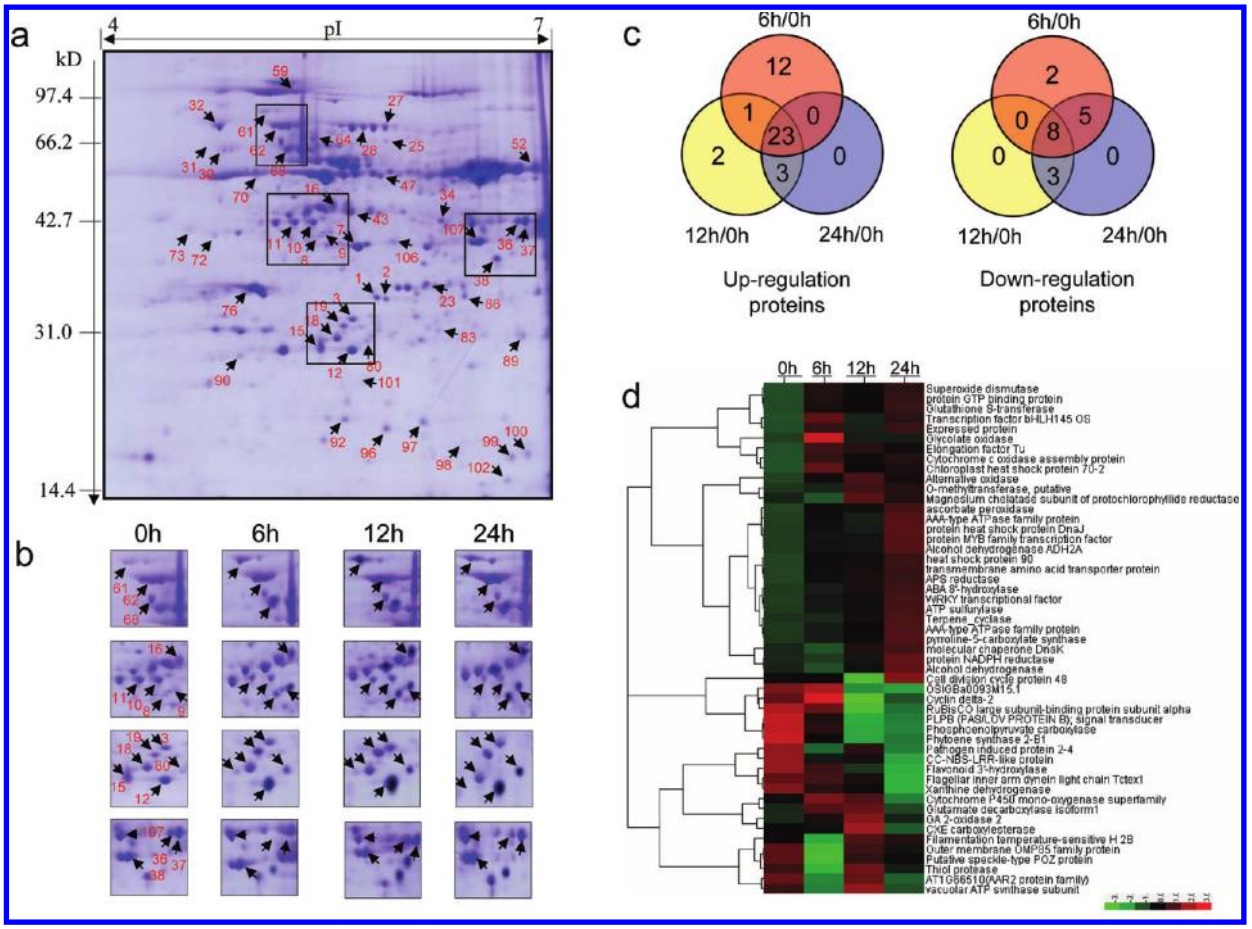

Figure 2. Fluctuations in protein expression in *P. oleracea* leaves following exposure to combined high temperature and high humidity. Three-week-old *P. oleracea* seedlings were exposed to 35 °C and 90% relative humidity for the indicated times. Total proteins (1 mg/sample) were extracted from leaves at different times during treatment and were examined by 2DE. (a) Representative CBB -stained 2D gel of total proteins extracted from leaves of plant seedlings treated with combined high temperature and high humidity for 24 h. (b) The enlarged window represents time-dependent changes in protein expression following combined temperature and humidity stressors. (c) Venn diagram of differentially expressed proteins following treatment. (d) Hierarchical clustering of the *P. oleracea* protein expression profile following temperature and humidity stressors. Cluster analyses were conducted using Cluster 3.0 and Treeview open source software (http://bonsai.ims.u-tokyo.ac.jp/~mdehoon/software/cluster). Different colors correspond to the proteins' log-transformed fold-change ratios depicted in the bar at the bottom of the figure.

primary antibodies and then with horse radish peroxidase-conjugated goat anti-rabbit secondary antibody (Promega). Signals were detected colorimetrically using an ECL Advance Western Blotting Detection kit, per the manufacturer's instructions (GE Healthcare, Knox, IN). Polyclonal primary antibodies (Agrisera) were diluted as follows: anti-P5CS, 1:2000; anti-HSP, 1:3000; and anti-actin, 1:3000. Anti-ABA-8′-hydroxylase antibody was prepared by immunizing a rabbit with synthesized peptides from *Arabidopsis* ABA-8′-hydroxylase (CYP707A2, sequence FPVPKKGLPIRVTPI).

RESULTS AND DISCUSSION

Different Physiological Responses in Thermotolerant *P. oleracea* and Thermosensitive *A. thaliana* under High-Temperature and High-Humidity Stress

We first compared the effects of various temperatures and humidity levels on the viabilities of *P. oleracea* and *A. thaliana*. The leaf MDA value and extent of ion leakage are the primary indicators reflecting the plasma membrane lipid oxidative damage.[24] We found that *P. oleracea* could tolerate temperatures exceeding 35 °C and a relative humidity of 90%, as evidenced by low MDA levels and negligible ion leakage under these conditions (Figure 1). In contrast, *A. thaliana* scarcely survived these conditions and exhibited high MDA levels and significant ion leakage after 3 d (Supporting Information Figure 1). Increasing the ambient humidity aggravated the negative effect of high temperatures on plant viability in *A. thaliana*, whereas *P. oleracea* tolerated high temperatures and high humidities (Supporting Information Figure 1). To confirm the thermal tolerance of *P. oleracea*, plants were grown under controlled conditions of 35 °C, the temperature at which half of the *A. thaliana* plants died, and 90% humidity. *P. oleracea* leaves remained greenish and vigorous after 96 h of 35 °C and 90% humidity, whereas *A. thaliana* leaves turned yellowish and wilted during this period (Figure 1a).

We then compared the maximum photochemical efficiencies of PS II in the dark-adapted state (F_v/F_m), which reflects the plants' photosynthetic capabilities. Elevated temperature and humidity significantly decreased the F_v/F_m of *A. thaliana*, whereas the F_v/F_m ratio remained high in *P. oleracea* (Figure 1). Exposure to heat and humidity significantly depleted the chlorophyll content of *A. thaliana* but not *P. oleracea* (Figure 1b). *A. thaliana* also exhibited a significant increase in MDA content following thermal and humidity stress (Figure 1b). In *P. oleracea*, the transpiration rate and stomata conductance

dx.doi.org/10.1021/pr300027a | J. Proteome Res. 2012, 11, 3605−3623

Table 1. MS Identification of Differentially Expressed Proteins in *P. oleracea* under Combined High-Temperature and High-Humidity Stress

spots no.	NCBI accession no.[a]	protein name	organism	theo. M_w/pI[b]	exp. M_w/pI[c]	score[d]	SC[e]	p-value[f]	sequence	ratio 6 h/0 h	ratio 12 h/0 h	ratio 24 h/0 h
					Energy and Metabolism Pathway							
1	gil255561094	vacuolar ATP synthase subunit	*R. communis*	39.8/5.36	37.7/5.77	125	14.04%	0.03	CTVK DVQELLEK AYLEDFYR AFYEEEVK YPPYQSIFAK NLMWISECVAQNQK	−1.90	2.31	−1.57
2	gil1323748	Thiol protease	*T. aestivum*	41.4/6.76	37.1/5.84	156	14.17%	0.04	FHGWMAK LQEHAATIR SINWVNQSK NVEFIEAANR NGGIANSSTYPYK	−3.23	2.5	−1.22
3	gil82697979	CXE carboxylesterase	*A. chinensis*	38.1/5.45	32.5/5.60	112	11.66%	0.02	TAQETQK VFDDGSVDR IYLPDTADYEK LAGAIPIHLGFVR	1.10	2.60	−1.03
7	gil1041248	pyrroline-5-carboxylate synthase	*A. thaliana*	77.7/5.89	41.7/5.69	194	11.85%	0.01	QLNETVK AFARDVK ACDTDMAK SFNHEYCAK VGTAVVTGK VGTLFHQDAR TEVADGLVLEK QLVNSSFADLQK GPVGVEGLLTTR	1.46	2.01	2.52
8	gil6606509	ATP sulfurylase	*A. thaliana*	51.4/6.30	42.0/5.40	89	10.15%	0.02	IGESTR HEAADLPR TPFLSQPLTK AGLIAPDGGK PYSFASSVSGFTK	2.54	5.76	7.75
9	gil2098778	APS reductase	*A. thaliana*	50.8/6.11	42.1/5.46	99	11.65%	0.04	YPSEHR AWITGQR SGASSESK EEDGAADSK ASTLIAPEVEEK LEDASPLEIMDK	3.37	7.94	9.30
10	gil160690008	Xanthine dehydrogenase	*T. chantieri*	46.9/6.74	42.8/5.40	103	11.59%	0.01	CTGYR FQITDCK TMPLHLR TEDSLYTR GLEIGASVR	−1.41	−1.17	−3.96

dx.doi.org/10.1021/pr300027a | *J. Proteome Res.* 2012, 11, 3605−3623

Table 1. continued

spots no.	NCBI accession no.[a]	protein name	organism	theo. M_w/pI[b]	exp. M_w/pI[c]	score[d]	SC[e]	p-value[f]	sequence	ratio 6 h/0 h	ratio 12 h/0 h	ratio 24 h/0 h
					Energy and Metabolism Pathway							
15	gil109390037	Phytoene synthase 2-B1	*T. turgidum*	28.8/5.47	30.3/5.39	143	14.17	0.02	EDDIALVNAGMR GKVTDK FPIDIQPFR AVWAIYVWCR GVMHLDSASR	−3.96	−5.36	−8.67
16	gil341869947	ABA 8′-hydroxylase (Cry702A)	*A. thaliana*	35.8/6.79	41.5/5.40	155	3.38%	0.02	FVLVTK ERMLGK ELAEILNK VASVLSFTFR DTTASVLTWIVK	3.96	9.64	12.36
34	gil115448583	AAA-type ATPase family protein	*O. sativa*	58.1/5.43	42.0/5.92	231	10.5%	0.04	FETNR LVGQK GGFSLR DSEMHEATR TISDLEGMGVR PAAASPSHALGSR GMPHGSYPQFDVAVK	1.96	3.42	4.67
43	gil50726339	ATPase family protein	*O. sativa*	56.7/5.37	49.2/5.67	210	7.5%	0.03	ALESPK GGAMDAR IFVFTTNHIEK HPSTFDTLAMDPER	1.96	3.42	4.68
47	gil115443611	transmembrane amino acid transporter protein	*O. sativa*	62.6/5.9	69.5/5.70	144	10.3%	0.03	YASEEER YANIIMLR SSQYLLPSR TPEILSNLVK LSNSFLTNSFR VAVWTTVANPITK	2.70	5.15	6.25
52	gil283896782	Phosphoenolpyruvate carboxylase	*C. dactylon*	57.0/6.62	57.8/6.73	95	9.94%	0.03	ANYEETK VVPLFEK SIVFEEPR PLFGPDLPR FSAAWQLYK FHLPVWLGFR	−1.64	−2.15	−2.85
70	gil116309564	Terpene_cyclase	*O. sativa*	53.9/5.18	57.2/5.12	233	21.2%	0.02	DILR FYEIILR EIETALK YLAAFSK APLADQVK VTADVAIAR	1.91	4.30	5.96

dx.doi.org/10.1021/pr300027a | *J. Proteome Res.* 2012, 11, 3605−3623

Table 1. continued

spots no.	NCBI accession no.[a]	protein name	organism	theo. M_w/pI[b]	exp. M_w/pI[c]	score[d]	SC[e]	p-value[f]	sequence	ratio 6 h/0 h	ratio 12 h/0 h	ratio 24 h/0 h
					Energy and Metabolism Pathway							
									GFWVSPDIFNK			
									DVLAYMGLDHIR			
									LDFNLLQQVHLK			
									QLQEVPEDLYVK			
									PSFNDQVALGTATTGTR			
73	gil171854577	Glutamate decarboxylase isoform1	*S. lycopersicum*	56.7/5.88	41.1/4.82	154	8.76%	0.04	LGFEGYK	3.21	5.54	1.53
									LIMSSINK			
									YVQEPLPK			
									ILSELDTQPPR			
									EGYYVMDPAK			
83	gil219551887	Flavonoid 3′-hydroxylase	*I. lobata*	31.1/6.02	31.07/5.98	178	13.03%	0.03	TPVK	−1.36	−1.47	−3.34
									LTDIEIK			
									INGYFIPK			
									VFNDGGSK			
									DVDFLSTLLR			
98	gil66730860	Glycolate oxidase	*S. ycopersicum*	16.7/8.84	15.1/6.24	192	19.08%	0.04	SLSWK	2.60	1.93	1.59
									EADIKNR			
									FFQLYVYK			
									NFEGLDIGK			
100	gil255577856	O-methyltransferase, putative	*R. communis*	13.1/5.60	14.7/6.72	107	20.91%	0.01	LEYDR	1.97	5.73	4.31
									EWEYVLQK			
									CKEAVPEDNR			
106	gil51011366	GA 2-oxidase 2	*N. oleander*	37.4/7.01	40.8/5.72	166	7.83%	0.04	LADNR	1.35	1.88	2.27
									PDSKHLLVK			
									SNNTSGLQIQLK			
					Defense Response							
11	gil255577887	Alcohol dehydrogenase	*R. communis*	30.5/6.12	43.6/5.26	213	17.88%	0.02	EEITGLPK	−1.41	−1.17	−3.96
									MLDPVLLNIR VIDSGSPDFK			
									LGFDDAFNYK			
									NLYLSCDPYMR			
12	gil119388745	Alcohol dehydrogenase ADH2A	*T. turgidum*	40.8/5.81	42.9/5.72	210	15.04%	0.03	GEGLR	1.2	1.96	2.68
									ELDVEK			
									MSGASR			
									INPEAPLDK			
									AAVAWEAGK			
									GVMIGDGESR			
									SEESNLCDLLR			
37	gil115436952	protein heat shock protein DnaJ	*O. sativa*	44.9/6.11	42.9/6.89	113	15.6%	0.02	YHPDK	2.93	4.83	10.02

dx.doi.org/10.1021/pr300027a | *J. Proteome Res.* 2012, 11, 3605−3623

Table 1. continued

spots no.	NCBI accession no.[a]	protein name	organism	theo. M_w/pI[b]	exp. M_w/pI[c]	score[d]	SC[e]	p-value[f]	sequence	ratio 6 h/0 h	ratio 12 h/0 h	ratio 24 h/0 h
				Defense Response								
61	gil225903795	heat shock protein 90	*Z. mays*	80.0/5.00	80.2/5.18	185	10.62%	0.03	LGVPIK QFETEYR DPEAAFFK WFNLNLNR VTSAAQSK MEGPSAPAMR PLPVGSSATGK EIFLR MTLYLK VVVTTK VVVSDR FESLTDK FYEAFSK EEYAAFYK DYVTRMK EISDDEDEEDK DSSMSGYMSSK	5.77	14.75	20.98
62	gil187830110	Filamentation temperature-sensitive H 2B	*Z. mays*	72.5/5.69	76.2/5.23	155	10.49%	0.04	TSDAR EIDDSIDR FLEYLDK IVEVLIEK GVLPFSAR QDFMEVVEFLK ALADEQGVSSSR	−1.29	2.10	1.72
64	gil30691626	molecular chaperone DnaK	*A. thaliana*	73.1/5.51	72.0/5.47	147	11.29%	0.03	GVLLVGPPGTGK EAAEK EQNITIR NTTIPTK VIENAEGSR EVQMASVSAFK TAMAGEDVEDIK APNGDAWVEANGQK	1.47	5.25	6.24
97	gil195626300	Pathogen induced protein 2−4	*Z. mays*	20.4/5.55	18.0/5.79	162	21.51%	0.04	ETGDR LKPAAVILGTR ELMEDLAVEAFK HAFDWALGHIAR	−3.02	−1.02	−3.55
				Chloroplast Related								
28	gil116308876	OSIGBa0093M15.1	*O. sativa*	76.1/5.08	76.8/5.63	149	5.12%	0.02	LLGEK MMMESVDLK	1.01	−1.08	−2.17

dx.doi.org/10.1021/pr300027a | *J. Proteome Res.* 2012, 11, 3605−3623

Table 1. continued

spots no.	NCBI accession no.[a]	protein name	organism	theo. M_w/pI[b]	exp. M_w/pI[c]	score[d]	SC[e]	p-value[f]	sequence	ratio 6 h/0 h	ratio 12 h/0 h	ratio 24 h/0 h
				Chloroplast Related								
31	gil134101	RuBisCO large subunit-binding protein subunit alpha	*R. communis*	52.3/4.77	66.9/4.93	159	10.51%	0.04	GVMGAVVEAK MELGALVEAK LICEFENAR LSGGVAVIK VVNEGVTIAR LADAVGLTLGPR EWEIGYNAMTDK	1.12	1.30	1.45
32	gil166919372	Chloroplast heat shock protein 70−2	*I. nil*	74.6/5.24	76.3/4.98	199	8.00%	0.03	GVPQIEVK IAGLEVLR IPAVQELVK LDCPAIGK PTIVTNAEGQR DAISGGSTQAMK	3.50	3.59	3.30
76	gil224179515	Magnesium chelatase subunit of protochlorophyllide reductase	*Msp. OKE-1*	38.5/5.22	37.8/5.17	158	13.83%	0.03	STTVR GDIVTNR DPLESIDTGTK LALILNVIDPK ITMVDLPLGATEDR	1.19	2.71	2.09
102	gil159480938	Cytochrome c oxidase assembly protein	*C. reinhardtii*	10.3/6.07	14.1/6.55	145	27.42%	0.02	GPDSGNLR MSAAFGGPR DLMAQQDLK	10.07	15.14	15.75
				Antioxidant Enzyme								
18	gil300693041	Glutathione S-transferase	*Z. jujube*	25.2/6.10	31.1/5.57	173	17.57%	0.03	DGETR VELALK ETLPPHDK LLPDDFYER PYFLSINPVYK	1.83	2.25	2.89
68	gil115475499	protein NADPH reductase	*O. sativa*	78.6/5.13	64.6/5.28	160	13.6%	0.02	ALAEEAK GVCSTWIK QYEHFNK QSGAELGR WFTEGNER PDEAAHLER EYVQHKMSQK ETLWPELDQLLR LLGYSPEAFFTIHADK	1.40	2.40	3.79
80	gil217833	ascorbate peroxidase	*A. thaiana*	27.5/5.72	28.4/5.95	166	13.56%	0.02	GLIAEK LPDATK GMGLSDK	5.34	10.44	12.35

dx.doi.org/10.1021/pr300027a | *J. Proteome Res.* 2012, 11, 3605−3623

Table 1. continued

spots no.	NCBI accession no.[a]	protein name	organism	theo. M_w/pI[b]	exp. M_w/pI[c]	score[d]	SC[e]	p-value[f]	sequence	ratio 6 h/0 h	ratio 12 h/0 h	ratio 24 h/0 h
					Antioxidant Enzyme							
90	gil488826	Alternative oxidase	*M. indica*	31.5/7.16	28.5/5.12	185	10.95%	0.02	ALLDDPVFR YGCR DATLK HHVPR TVKILR	4.43	14.28	6.85
96	gil311323686	Cytochrome P450 mono-oxygenase superfamily	*P. mariana*	24.0/6.64	15.1/5.84	194	14.29%	0.02	ALLEEAENER ETLR NPLQASIK MMPFGVGR	4.94	8.05	7.56
101	gil332659607	Superoxide dismutase	*A. thaliana*	23.7/6.06	26.45/5.90	192	16.04%	0.03	DGETPDISEK PDYIK PGGGGK DFTSYEK AYVDNLK QTLEFHWGK	8.16	14.38	18.02
					Cell Division and Structure							
19	gil111117309	Elongation factor Tu	*C. racemosa*	26.2/5.32	32.7/5.57	147	13.33%	0.03	DPWVDK IDQVDDK FQAQVYILK GTVATGRVER	2.17	2.68	2.10
23	gil253721995	Putative speckle-type POZ protein	*A. tauschii*	29.1/6.41	37.3/5.81	184	10.69%	0.04	YNVVR CVLAAR CDVTVMK ILPAEWSVAK	−4.56	1.49	1.81
27	gil297806563	Outer membrane OMP85 family protein	*A. lyrata*	58.5/6.22	76.4/5.78	184	7.06%	0.03	AEAR QEHDR FLETFR EDAIADR FSSYKER GLGPNESR	−3.38	1.44	−1.32
59	gil110289141	Cell division cycle protein 48	*O. sativa*	89.8/5.09	101.3/5.39	211	15.5%	0.03	LQLFR QMAQIR FGMSPSK IHTKNMK PYFLEAYR DYSTAILER LTALKKPFK PDIIDPALLR YQAFAQTLQQSR	2.08	−1.06	−1.48

dx.doi.org/10.1021/pr300027a | *J. Proteome Res.* 2012, 11, 3605−3623

Table 1. continued

spots no.	NCBI accession no.[a]	protein name	organism	theo. M_w/pI[b]	exp. M_w/pI[c]	score[d]	SC[e]	p-value[f]	sequence	ratio 6 h/0 h	ratio 12 h/0 h	ratio 24 h/0 h
				Cell Division and Structure								
86	gil227202636	AT1G66510 (AAR2 protein family)	*A. thaliana*	25.2/6.45	26.7/6.72	156	8.58%	0.03	SLEFDK ALELVK VSEEEEER	−1.68	2.28	−1.58
99	gil303287168	Flagellar inner arm dynein light chain Tctex1	*M. pusilla*	11.7/7.71	15.4/6.70	204	12.26%	0.04	WENK LTALKKPFK	−1.06	1.15	2.29
107	gil1076312	Cyclin delta-2	*A. thaliana*	42.9/5.20	40.7/6.38	159	12.5%	0.03	FVFEAK FILNTTK IKEMLVR QEEEKTMR ALSSLIYVK LLSGDLDLSVR	1.15	−1.32	−1.52
				Transcriptional and Signal Transduction								
30	gil297612820	protein GTP binding protein	*O. sativa*	87.4/6.68	65.7/4.91	173	13.8%	0.03	DWISYR HVEALQIK VQLVGNAGR LLAEANSLLK SAYLDELDYR YLITDDMVFR SPPDIVLYFER SATINSIFDEPK EDLYIQSECSVSYSGK TGVPPTTDVVAQVLYR	2.29	3.95	4.81
36	gil46394386	WRKY transcriptional factor	*O. sativa*	51.7/5.15	42.9/6.88	127	12.5%	0.04	GYYR QVERSR GAVGGIK EYMATNYK AIRPYPVMAGDTVK TSGEVVPSDLWAWR	2.22	4.21	5.26
38	gil297722033	protein MYB family transcription factor	*O. sativa*	32.3/5.76	39.4/6.61	155	13.0%	0.04	PPCCDK YTNYLR NYWNTK GIDPITHR GPWTAEEDAK WSLIANQLPGR	2.20	3.48	5.54
72	gil75170387	Transcription factor bHLH145 OS	*A. thaliana*	34.7/5.08	41.1/4.85	193	9.32%	0.03	EELQR SFETLK AEEQCSQK ILETSNESMR	1.82	1.69	2.92
89	gil42570655	PLPB (PAS/LOV PROTEIN B); signal transducer	*A. thaliana*	40.5/6.47	31.4/6.71	182	8.94%	0.03	LVCGKR	−2.57	−3.98	−5.92

dx.doi.org/10.1021/pr300027a | *J. Proteome Res.* 2012, 11, 3605−3623

Table 1. continued

spots no.	NCBI accession no.[a]	protein name	organism	theo. M_w/pI[b]	exp. M_w/pI[c]	score[d]	SC[e]	p-value[f]	sequence	ratio 6 h/0 h	ratio 12 h/0 h	ratio 24 h/0 h
				Transcriptional and Signal Transduction								
92	gil47027824	CC-NBS-LRR-like protein	*H. annuus*	25.4/6.40	17.8/5.67	167	11.16%	0.03	YTLWIK SIMEIREAIR SVQVSLLNYR TTLAR AQGIHNELK INRDLENLEKR	−1.31	−1.06	−1.68
				Unknown Proteins								
25	gil77552210	Expressed protein	*O. sativa*	67.4/7.31	70.8/5.76	159	7.79%	0.03	VDAIPR MAVVQR ASLLAVER VAVPATAAR VTDAFAACVR CVEMDMIEER	2.39	2.38	3.14

[a]Database accession numbers according to NCBInr. [b]Theoretical M_w/pI. [c]Experimental M_w/pI. [d]The Mascot search score against the database of NCBInr. [e]Sequences coverage. [f]Protein spots showed a significant change in abundance (fold change) by a factor >1.5-fold compared to the control analyzed by LSD test. A p-value of <0.05 was considered statistically significant.

dx.doi.org/10.1021/pr300027a | *J. Proteome Res.* 2012, 11, 3605−3623

levels increased following high-temperature and high-humidity treatments. Similar increases in transpiration rate and stomatal conductance were recorded in *A. thaliana* during the first 12 h of treatment, but those parameters dropped rapidly in subsequent hours, reflecting substantial damage to seedling leaves (Figure 1b). These results demonstrate the enhanced potential of *P. oleracea* to tolerate high-temperature and high-humidity stressors.

Identification and Functional Classification of Potential Thermotolerance Proteins in *P. oleracea* Using MALDI-TOF/TOF

To explore the underlying mechanism of *P. oleracea* tolerance to elevated temperature and humidity, the *P. oleracea* leaf proteome was analyzed by 2DE. Representative gels from samples collected after 6, 12, and 24 h of treatment are shown in Figure 2a,b and in Supporting Information Figure 2. Approximately 154 protein spots reproducibly exhibited significant changes in response to stress treatments ($p < 0.05$). Of these, 51 proteins, corresponding to 7 putative classes of biological functions, were identified by MALDI-TOF/TOF. The majority of the proteins corresponded to material and energy metabolism, followed by antioxidant enzymes, defense-response proteins, transcription factors, chloroplast-related proteins, proteins involved in cell structure, and unknown proteins (Figure 2, Table 1, Supporting Information Table 1). In total, 23 proteins were globally increased throughout the exposure period of 6−24 h, whereas 8 proteins were decreased (Figure 2c). A hierarchical cluster analysis was conducted to examine proteins showing similar expression profiles during high-temperature and high-humidity stress (Figure 2d). We observed that proteins belonging to the antioxidant system clustered together. Specifically, proteins involved in proline or ABA metabolism were increased, supporting that they contribute to *P. oleracea* tolerance during combined high-temperature and high-humidity stressors.

Material- and Energy-Associated Proteins Primarily Control Thermal Tolerance in *P. oleracea*

The carbon pool is largely used for the synthesis of storage/structural polysaccharides, whereas nitrogen pools contribute to amino acid and nucleotide synthesis and are the basis for material and energy metabolism in the cell. In the present study, carboxylesterase (Figure 2a, spot 3) and phosphoenolpyruvate carboxylase (Figure 2a, spot 52), which are involved in carbon fixation during photosynthesis, were differentially regulated in the leaves of *P. oleracea* during conditions of elevated temperature and humidity. Glycolate oxidase (GOX, Figure 2a, spot 98) was increased in response to our stress treatment, with peak expression during the first 6 h of exposure. GOX represents a major constituent of the peroxisomal matrix in photosynthetic tissues. As such, GOX is a key enzyme involved in the photorespiratory pathway, facilitating the dissipation of excessive energy and protecting photosynthetic membranes.[32,33] Transgenic Pssu-ipt tobacco expressing higher levels of GOX are more tolerant to heat stress than nontransformed control plants.[34] These results support our findings and indicate that a higher photorespiration rate contributes to combined heat and humidity tolerance in *P. oleracea*.

Xanthine dehydrogenase (XDH), a molybdenum-cofactor protein, is involved in purine catabolism, nucleotide synthesis, amino acid binding, and the stress response.[34−36] XDH increase facilitates plant survival by assisting in oxidation−reduction processes involved in heat stress responses under the influence of cytokinins.[34] XDH also protects plant tissue from cold-associated oxidative stress. We observed the reduction of XDH (Figure 2a, spot 10) under high-temperature and high-humidity conditions.

Glutamate decarboxylase isoform1 (Figure 2a, spot 73), a protein associated with amino acid biosynthesis, was increased in *P. oleracea* during conditions of elevated temperature and humidity.[37,38] Similarly, *O*-methyltransferase (Figure 2a, spot 100), an important enzyme linking carbon and nitrogen metabolism, was induced following our thermal stress treatment. These findings suggest that carbon and nitrogen resources are quickly transformed in *P. oleracea* with exposure to high heat and humidity.[39] Our stress protocol induced a rapid accumulation of certain proteins involved in sulfur metabolism, including ATP sulfurylase (ATPS, Figure 2a, spot 9), 5′-adenylylsulfate (APS) reductase (Figure 2a, spot 8), and thiol protease (i.e., cysteine protease, Figure 2a, spot 2). Heat stress and wounding treatment induce the accumulation of cysteine proteinase in rice leaves[22] and tobacco.[40] These observations support that extreme temperatures and humidities evoke responses comparable to those elicited by other stresses; that is, stress-response pathways appear to be linked. ATPS catalyzes the activation of sulfate by binding to AMP and synthesizing APS. In the present study, the increase of ATPS (2.4- to 7.8-fold) during the first 6−24 h of heat and humidity stress suggests that APS synthesis is increased, which would promote cysteine synthesis. As the final product of the sulfate reduction pathway, cysteine donates a sulfur to methionine[41] and is part of GSH, which removes toxic metabolites from the cell while preventing oxidation of sulfhydryl groups. Increase of ATPS at the mRNA and protein levels has been observed in heat-stressed *P. euphratica*.[42] Several proteins involved in plant secondary metabolism, such as flavonoid 3′-hydroxylase (Figure 2a, spot 83) and phytoene synthase 2-B1 (Figure 2a, spot 100), were decreased throughout exposure. This indicates an inhibition of secondary metabolite synthesis (e.g., flavonoids and carotenoids) in plants exposed to combined high-temperature and high-humidity stressors.

Other proteins related to energy production and conversion, such as vacuolar ATP synthase (V-ATPase, Figure 2a, spot 1) and an AAA-type ATPase family protein (Figure 2a, spot 34), were differentially regulated upon exposure in *P. oleracea*. V-ATPase was decreased during both short-term (6 h) and long-term (24 h) stress exposure. However, V-ATPase was increased at 12 h of exposure. V-ATPase establishes and maintains an electrochemical proton gradient across the tonoplast, providing the driving force for the active transport of metabolites and ions. This enzyme is known to be of central importance in plant responses to salt,[43] metal stress,[44] and heat stress.[45] Increased V-ATPase activity also may serve a homeostatic function to maintain the cytoplasmic pH near neutrality. The 1.9- to 4.7-fold increase in the AAA-type ATPase family protein observed during 6−24 h of exposure was closely correlated with an increase in the level of ribulose biphosphate carboxylase oxygenase (RuBisCO) activase, which belongs to the AAA+ family (ATPase associated with diverse cellular activities) involved in the regeneration of carbamylated active sites in RuBisCO to maintain its activity.[46] The accumulation of RuBisCO activase (Figure 2a, spot 34) during elevated temperature and humidity conditions suggests a greater photosynthetic CO_2 fixation capability via RuBisCO activity in *P. oleracea*. A positive correlation between the heat stability

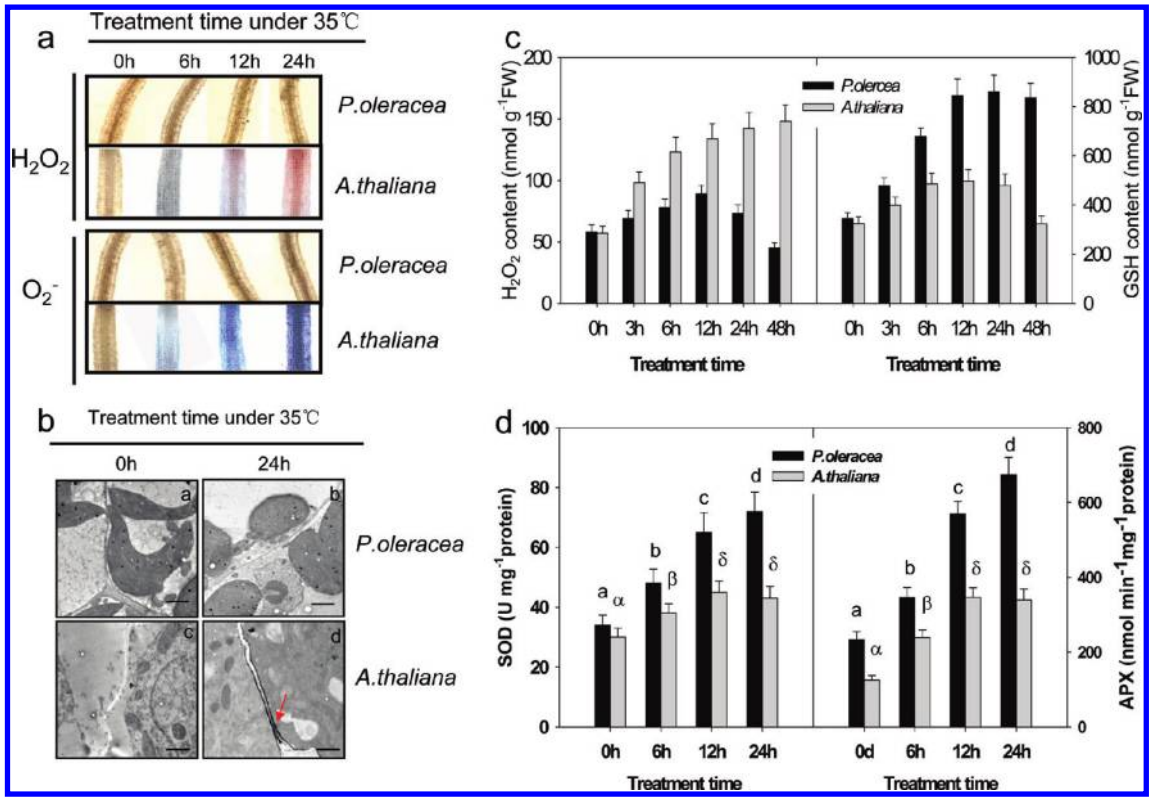

Figure 3. Effects of combined temperature and humidity on ROS (H_2O_2 and O_2^-) and antioxidant activity in seedling leaves. (a) *In situ* detection of H_2O_2 (upper) and O_2^- (lower) generation in *P. oleracea* and *A. thaliana* following combined high-temperature and high-humidity stresses. One-week-old *P. oleracea* and *A. thaliana* seedlings were exposed to 35 °C and 90% relative humidity for the indicated times, and H_2O_2 and O_2^- were measured by reported method. (b) Cytochemical localization of stress-induced H_2O_2 in *P. oleracea* leaves using TEM detection of $CeCl_3$ deposits. Bar = 100 μM. (c) Time course of H_2O_2 and GSH content following temperature and humidity stressors in *P. oleracea* and *A. thaliana* leaves. (d) Time course of SOD and APX activities following temperature and humidity stressors in *P. oleracea* and *A. thaliana* leaves.

of RuBisCO activase and the heat tolerance of plants from contrasting thermal environments has recently been reported.[46,47]

The Accumulation and Increased Activity of Antioxidants Efficiently Remove ROS Toxicity in *P. oleracea* under Conditions of High Temperature and Humidity

A consistently higher level of glutathione *S*-transferase (GST, Figure 2a, spot 18) throughout the exposure duration (6−24 h) indicates that the GSH−ascorbate cycle actively participates in maintaining the redox status within appropriate levels.[21,22] GST is an abundant protein that catalyzes the conjugation of reduced GSH to detoxify endogenous compounds. GST may function in GSH−ascorbate cycles with regard to antioxidant metabolism. Recent studies have suggested that GSTs are components of ultraviolet-inducible cell signaling pathways and are potential regulators of apoptosis.[48] Increased GST expression has been reported in *Agrostis scabra* following exposure to thermal stress.[49] The elevated GST levels observed in *P. oleracea* may lead to depleted active oxygen species, resulting in superior thermal and humidity tolerance. In addition, SOD (spot 101), which is involved in O_2^- detoxification; APX (Figure 2a, spot 80), which minimizes H_2O_2 accumulation; and a cytochrome P450 superfamily protein (Figure 2a, spot 96), which effects oxidation of organic substances and plant defense responses,[50] were significantly increased in *P. oleracea* after 12- and 24-h exposures to high temperature and high humidity. SOD functions as the first line of defense against stress, converting O_2^- to the less toxic H_2O_2. During heat stress, the thermotolerant *A. scabra* expressed more SOD and peroxidases than thermosensitive *Agrostis stolonifera*.[49] A comprehensive transcriptome analysis coupled with a phenotype analysis of T-DNA insertional mutants in *Arabidopsis* revealed that cytosolic APX plays a key role in heat acclimation in conjunction with heat-shock transcription factors.[51]

To compare the functions of the antioxidant systems of *P. oleracea* and *A. thaliana* subjected to thermal and humidity stressors, we measured the *in situ* generation of H_2O_2 and O_2^- using diaminobenzidine tetrahydrochloride (DAB) and nitro-blue tetrazolium (NBT) staining. High temperature and humidity accelerated the production of H_2O_2 and O_2^- in *A. thaliana* (6 h), and sustained substantial ROS production even after 24 h of treatment (Figure 3a). However, such exposure did not induce ROS accumulation in *P. oleracea* (Figure 3b). In addition, $CeCl_3$-based histochemical detection demonstrated that H_2O_2 amassed in the intracellular spaces of *A. thaliana* but accumulated to a much lesser degree in *P. oleracea* (Figure 3c). We also measured a 10-fold increase in chloroplast size in *P. oleracea* compared with *A. thaliana*; this suggests augmented photosynthetic performance and/or an enhanced capability for material and energy synthesis in *P. oleracea* exposed to stress (Figure 3c). In agreement with protein expression analyses, the enzyme activities of APX and SOD also increased in *P. oleracea* under high-temperature and high-humidity conditions compared with the activities of these enzymes in *A. thaliana* (Figure 3d). GSH is an extremely efficient ROS scavenger across diverse environmental conditions.[22,23] We measured consistently elevated GSH in heat and humidity-exposed *P. oleracea* (Figure 3c). In contrast, *A. thaliana* could not sustain high level

dx.doi.org/10.1021/pr300027a | *J. Proteome Res.* 2012, 11, 3605−3623

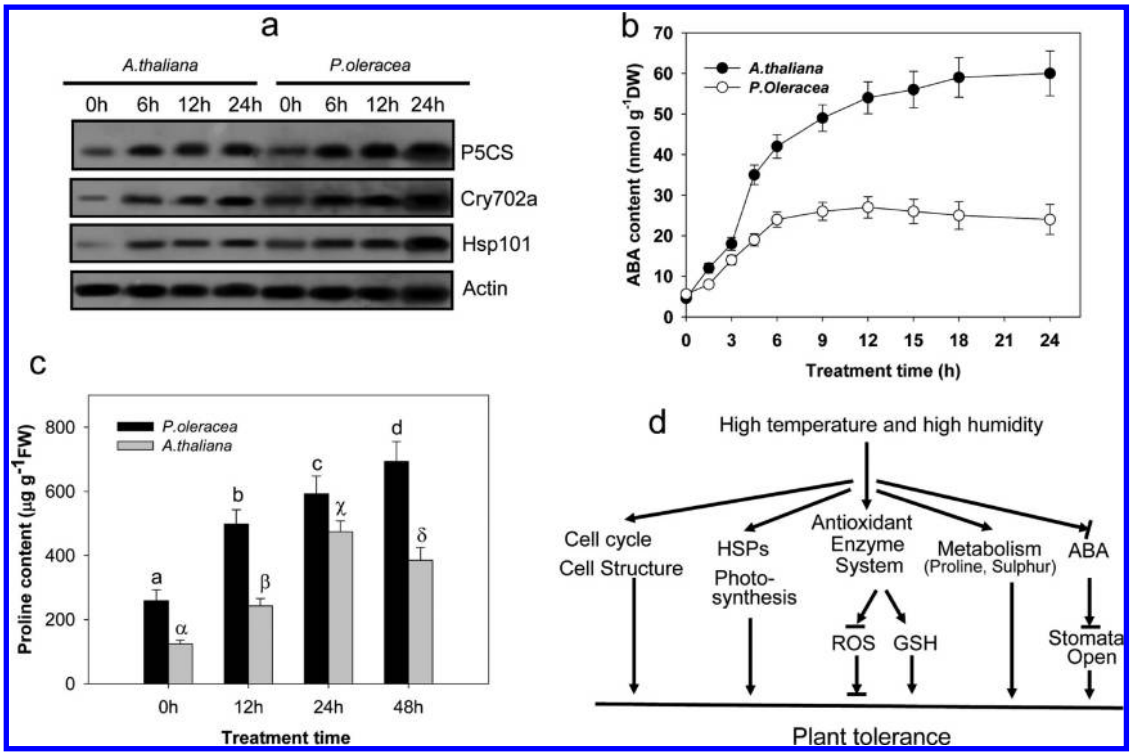

Figure 4. The effects of concomitant heat and humidity stressors on proline and the ABA metabolic pathway. (a) Accumulation of P5CS, ABA-8′-hydroxylase (Cry702a), and HSP101 in the leaves of *P. oleracea* and *A. thaliana* induced by exposure to 35 °C and 90% relative humidity. (b and c) Accumulation of proline (b) and ABA (c) in the leaves of *P. oleracea* and *A. thaliana* following stress treatment. (d) Proposed model demonstrating that *P. oleracea* applies multiple strategies in response to combined high-temperature and high-humidity stressors.

of GSH; this component decreased significantly after 48 h exposure, compared with GSH levels at 12 h. The substantially and consistently elevated levels of SOD, APX, GST, and GSH expressed by *P. oleracea* may suppress the production of ROS in this species and explain its superior heat and humidity tolerance.

Differential Expression Patterns of Stress-Responsive Proteins in *A. thaliana* and *P. oleracea*

Stress-responsive proteins, including alcohol dehydrogenases and pathogen-induced protein 2−4, were decreased in *P. oleracea* following exposure to high temperature and humidity. However, ABA-8′-hydroxylase (Cry702A, Figure 2, spot 16), P5CS (spot 7), and HSP101 accumulated more in exposed *P. oleracea* than in *A. thaliana*, as confirmed by Western blotting (Figure 4a). ABA-8′-hydroxylase, which rose 3.9- to 12.4-fold during the 6−24 h exposure period, contributes to the control of cytosolic ABA levels. The hormone ABA acts as a secondary messenger in the cell to trigger stomatal closure, thereby limiting water loss via transpiration. ABA also mobilizes a battery of genes that presumably protect the cell from oxidative damage in response to various environmental cues, such as drought, cold, and heat.[52] We observed significantly increased ABA-8′-hydroxylase activity and correspondingly decreased ABA in *P. oleracea* compared with *A. thaliana* leaves. This may explain the enhanced stomatal conductance and respiration rate of *P. oleracea* under high-temperature and high-humidity stress conditions.

In plant cells, abiotic stressors can alter the levels of free amino acids.[14,15] Proline is an important osmolyte in plants that functions in stress adaptation. P5CS, which catalyzes the rate-limiting step of proline biosynthesis from glutamate, was dramatically increased in response to high-temperature and high-humidity stressors in *P. oleracea*. This finding is consistent with a previous study suggesting that P5CS1 plays a critical role in the response of plants to abiotic stressors such as osmotic stress.[53] Taken together, these results suggest that the increased activity of ABA biosynthesis-related proteins, in conjunction with the accumulation of proline and P5CS, may produce thermal and humidity tolerance in *P. oleracea*.

Chloroplast-Associated and Other Heat-Shock/Chaperonin Proteins Involved in the Response of *P. oleracea* to High-Temperature and High-Humidity Stresses

TEM analysis indicated that the chloroplasts of *P. oleracea* leaves were at least 5-fold larger than those in *A. thaliana* leaves (Figure 3b). This finding may reflect a difference between C3 (e.g., *A. thaliana*) and C4 (e.g., *P. oleracea*) plants. During all exposure time-points, *P. oleracea* significantly increased the chloroplast-associated protein RuBisCO large subunit-binding protein (Figure 2a, spot 31), the magnesium chelatase subunit of protochlorophyllide reductase (Figure 2a, spot 76), and the cytochrome c oxidase (Figure 2a, spot 102) assembly protein. The RuBisCO large subunit-binding protein α subunit, a chaperone protein, exhibited a 1.4-fold increase in expression level after 24 h of elevated heat and humidity. This result supports the findings of Gammulla et al.,[54] who reported an increase in the abundance of this protein in rice grown at 44 °C for 3 d. Similarly, the abundance of this protein increased in wheat grown under drought- and heat-stress conditions.[55]

HSP70 (Figure2a, spot 32), HSP90 (Figure 2a, spot 91), GTP-binding protein (Figure 2a, spot 30), and the molecular chaperones DnaK and DnaJ (Figure 2a, spot 64) were increased in heat and humidity-exposed *P. oleracea*. Proper folding is a critical step in the generation of a functional protein. HSP90 proteins act as chaperonins with ATPase activities,

dx.doi.org/10.1021/pr300027a | *J. Proteome Res.* 2012, 11, 3605−3623

interacting with proteins involved in transcriptional regulation and signal transduction pathways.[45] HSP70 prevents protein aggregation and assists in the refolding of non-native proteins under both basal and stressed conditions. The expression of HSPs and chaperonins has been correlated with the acquisition of thermotolerance in many plant species.[49] The abundance of HSPs, along with the increased expression of the RuBisCO subunit-binding protein during combined temperature and humidity stressors, suggests that these proteins participate in the folding of newly synthesized proteins and in the stabilizing and refolding of denatured proteins upon stress. The GTP-binding nuclear protein (Ran) was increased in the present study, peaking after 24-h exposure to heat and humidity stress. Under normal growth conditions, this protein assists in the import and export of proteins and RNA from the nucleus, chromatin condensation, and cell cycle control.[56] However, its role in the plant stress response is less clear. Others have reported an increase in Ran abundance under salt and heat stressors.[57]

Proteins Involved in Gene Transcription or Cell Division Exhibit Different Expression Levels in *P. oleracea* Responding to High-Temperature and High-Humidity Stresses

Plant cells can alter their structures and division capacities to adapt to harsh environmental conditions. We identified several cell structural and division-related proteins that were decreased in response to high-temperature and high-humidity stresses in *P. oleracea*. Cell division cycle protein 48 (Figure 2a, spot 59) and cyclin delta-2 (Figure 2a, spot 105) were decreased in response to stress. Cell structure-related proteins, including the flagellar inner-arm dynein light-chain Tctex1 protein (Figure 2a, spot 107) and elongation factor Tu (EF-Tu, spot 19), exhibited different degrees of increasing in *P. oleracea* in response to high temperature and high humidity. The signal-transduction-related protein PLPB (Figure 2a, spot 89) also was decreased, suggesting that it may play a role in the transduction of high-temperature- or high-humidity-induced signals in *P. oleracea*. These results suggest that *P. oleracea* cells reduced division or proliferation rates in response to high-temperature and high-humidity stresses while strengthening cell wall structures to enhance the plant's tolerance to these stressors.

Certain specialized transcription factors are responsible for the protection of gene expression in plants subjected to stress. We measured an increase in bHLH145 (spot 72), one of these stress-protective components. This factor belongs to the bHLH transcriptional factor family and is involved in plant development and the environmental stress response.[58,59] The MYB transcriptional factor family also regulates the response of plants to abiotic stress.[40,58] We identified altered expression of a MYB transcription factor (Figure 2a, spot 38), a WRKY transcription factor (Figure 2a, spot 36), and EF-Tu (Figure 2a, spot 19) in exposed *P. oleracea*. The expression of EF-Tu genes is differentially regulated in heat-tolerant and heat-sensitive maize lines, and the relative levels of EF-Tu correlate with heat-stress capacity in maize.[60] These observations support a complex modulation of plant response to heat and humidity stressors via special transcription factors.

CONCLUDING REMARKS

Several studies have investigated the effects of high temperatures on plant growth and development. The combined effects of heat and humidity more closely approximate environmental conditions, but these are poorly understood. In the present study, we investigated the physiological and proteomic contributors to thermotolerance in *P. oleracea*. Unlike the thermosensitive plant, *A. thaliana*, *P. oleracea* enhanced its photosynthetic capability in response to high heat and humidity stressors. In addition, the *P. oleracea* antioxidant system efficiently scavenges toxic ROS, further enabling the plant to acquire energy and perform metabolism under stress. During thermal stress, transiently induced defense-response molecules, including HSPs and proline, accumulate to enhance protein stability. In addition, *P. oleracea* improves its stress tolerance via ABA-mediated regulation of stomatal conductance and respiration, thereby reinforcing cell structure and reducing cell division to avoid excess material and energy consumption. In conclusion, *P. oleracea* applies multiple strategies to survive under high-temperature and high-humidity stress conditions. Focused breeding strategies may allow the cultivation of crops adaptable to thermal stress via similar mechanisms.

ASSOCIATED CONTENT

Supporting Information

Supporting Information Figure 1, the effects of elevated temperature and humidity on the growth of *P. oleracea* and *A. thaliana*; Supporting Information Figure 2, the protein profile of *P. oleracea* leaves exposed to high temperature and humidity stressors as measured by 2D SDS-PAGE; Supporting Information Table 1, MALDI-TOF/TOF analysis of differentially expressed proteins in *P. oleracea* exposed to combined heat and humidity stressors. This material is available free of charge via the Internet at http://pubs.acs.org.

AUTHOR INFORMATION

Corresponding Author

*Address: Kunming Institute of Botany, No. 132 Lanhei Road, Heilongtan,Kunming, Yunnan, 650204, China. Tel.: +86-871-5223069. Fax: +86-871-5223398. E-mail: (X.H.) huxiangyang@mail.,kib.ac.cn or (Y.Y.) yangyp@mail.kib.ac.cn.

Author Contributions

‡These authors contributed equally to this work.

Notes

The authors declare no competing financial interest.

ACKNOWLEDGMENTS

This work was supported by the 100 Talents Program of the Chinese Academy of Sciences and by grants from the National Science Foundation of China (No. 30871704, No. 30971452 and No. 31170256). Y.Y. was supported by Major State Basic Research Development Program (2010CB951704). C.B. was supported by a grant from the French Ministry of Foreign and European Affairs (MAEE) in the frame of the Zhang Heng Program. J.C. was supported by the Natural Science Foundation of Jiangsu University (No. 09KJA220001).

REFERENCES

(1) Lobell, D. B.; Burke, M. B.; Tebaldi, C.; Mastrandrea, M. D.; Falcon, W. P.; Naylor, R. L. Prioritizing climate change adaptation needs for food security in 2030. *Science* **2008**, *319* (5863), 607−10.

(2) Jeon, M. W.; Ali, M. B.; Hahn, E. J.; Paek, K. Y. Photosynthetic pigments, morphology and leaf gas exchange during ex vitro acclimatization of micropropagated CAM Doritaenopsis plantlets

under relative humidity and air temperature. *Environ. Exp. Bot.* **2006**, *55* (1−2), 183−94.
(3) Tashiro, T.; Wardlaw, I. F. The response to high temperature shock and humidity changes prior to and during the early stages of grain development in wheat. *Funct. Plant Biol.* **1990**, *17* (5), 551−61.
(4) Otto, H. W.; Daines, R. H. Plant injury by air pollutants: Influence of humidity on stomatal apertures and plant response to ozone. *Science* **1969**, *163* (3872), 1209−10.
(5) Fiscus, E. L.; Booker, F. L.; Sadok, W.; Burkey, K. O. Influence of atmospheric vapour pressure deficit on ozone responses of snap bean (Phaseolus vulgaris L.) genotypes. *J. Exp. Bot.* **2012**, *63* (7), 2557−64.
(6) Horvath, E. M.; Peter, S. O.; Joët, T.; Rumeau, D.; Cournac, L.; Horvath, G. V.; Kavanagh, T. A.; Schafer, C.; Peltier, G.; Medgyesy, P. Targeted inactivation of the plastid ndhB gene in tobacco results in an enhanced sensitivity of photosynthesis to moderate stomatal closure. *Plant Physiol.* **2000**, *123* (4), 1337−1350.
(7) Wang, L.; Ma, H.; Song, L.; Shu, Y.; Gu, W. Comparative proteomics analysis reveals the mechanism of pre-harvest seed deterioration of soybean under high temperature and humidity stress. *J. Proteomics* **2012**, *75* (7), 2109−27.
(8) Huang, B.; Xu, C. Identification and characterization of proteins associated with plant tolerance to heat stress. *J. Integr. Plant Biol.* **2008**, *50* (10), 1230−37.
(9) Ahsan, N.; Donnart, T.; Nouri, M. Z.; Komatsu, S. Tissue-specific defense and thermo-adaptive mechanisms of soybean seedlings under heat stress revealed by proteomic approach. *J. Proteome Res.* **2010**, *9* (8), 4189−204.
(10) Vierling, E. The roles of heat shock proteins in plants. *Annu. Rev. Plant Biol.* **1991**, *42* (1), 579−620.
(11) Wang, W.; Vinocur, B.; Shoseyov, O.; Altman, A. Role of plant heat-shock proteins and molecular chaperones in the abiotic stress response. *Trends Plant Sci.* **2004**, *9* (5), 244−52.
(12) Lindquist, S.; Craig, E. A. The heat-shock proteins. *Annu. Rev. Genet.* **1988**, *22* (1), 631−77.
(13) Hartl, F. U.; Martin, J.; Neupert, W. Protein folding in the cell: the role of molecular chaperones Hsp70 and Hsp60. *Annu. Rev. Biophys. Biomol. Struct.* **1992**, *21* (1), 293−322.
(14) Katiyar-Agarwal, S.; Agarwal, M.; Grover, A. Heat-tolerant basmati rice engineered by over-expression of hsp101. *Plant Mol. Biol.* **2003**, *51* (5), 677−86.
(15) Wells, D. R.; Tanguay, R. L.; Le, H.; Gallie, D. R. HSP101 functions as a specific translational regulatory protein whose activity is regulated by nutrient status. *Genes Dev.* **1998**, *12* (20), 3236−51.
(16) Ashraf, M.; Foolad, M. R. Roles of glycine betaine and proline in improving plant abiotic stress resistance. *Environ. Exp. Bot.* **2007**, *59* (2), 206−16.
(17) Hare, P. D.; Cress, W. A. Metabolic implications of stress-induced proline accumulation in plants. *J. Plant Growth Regul.* **1997**, *21* (2), 79−102.
(18) Toh, S.; Imamura, A.; Watanabe, A.; Nakabayashi, K.; Okamoto, M.; Jikumaru, Y.; Hanada, A.; Aso, Y.; Ishiyama, K.; Tamura, N. High temperature-induced abscisic acid biosynthesis and its role in the inhibition of gibberellin action in Arabidopsis seeds. *Plant Physiol.* **2008**, *146* (3), 1368−85.
(19) Xuan, Y.; Zhou, S.; Wang, L.; Cheng, Y.; Zhao, L. Nitric oxide functions as a signal and acts upstream of AtCaM3 in thermotolerance in Arabidopsis seedlings. *Plant Physiol.* **2010**, *153* (4), 1895−906.
(20) Neill, S.; Desikan, R.; Hancock, J. Hydrogen peroxide signalling. *Curr. Opin. Plant Biol.* **2002**, *5* (5), 388−95.
(21) Anjum, N. A. *Ascorbate-Glutathione Pathway and Stress Tolerance in Plants*; Springer Verlag: Dordrecht, 2010.
(22) Foyer, C. H.; Noctor, G. Ascorbate and glutathione: the heart of the redox hub. *Plant Physiol.* **2011**, *155* (1), 2−18.
(23) Bai, X.; Yang, L.; Tian, M.; Chen., J.; Shi, J.; Yang, Y.; Hu, X. Nitric oxide enhances desiccation tolerance of recalcitrant *Antiaris toxicaria* seeds via protein S-nitrosylation and carbonylation. *PLoS One* **2011**, *6* (6), e20714.
(24) Zhang, M.; Li, G.; Huang, W.; Bi, T.; Chen, G.; Tang, Z.; Su, W.; Sun, W. Proteomic study of Carissa spinarum in response to combined heat and drought stress. *Proteomics* **2010**, *10* (17), 3117−29.
(25) Barbosa, H.; Slater, N. K. H.; Marcos, J. C. Protein quantification in the presence of poly (ethylene glycol) and dextran using the Bradford method. *Anal. Biochem.* **2009**, *395* (1), 108−10.
(26) Bernstein, N.; Shoresh, M.; Xu, Y.; Huang, B. Involvement of the plant antioxidative response in the differential growth sensitivity to salinity of leaves vs roots during cell development. *Free Radical Biol. Med.* **2010**, *49* (7), 1161−71.
(27) Ding, S.; Lu, Q.; Zhang, Y.; Yang, Z.; Wen, X.; Zhang, L.; Lu, C. Enhanced sensitivity to oxidative stress in transgenic tobacco plants with decreased glutathione reductase activity leads to a decrease in ascorbate pool and ascorbate redox state. *Plant Mol. Biol.* **2009**, *69* (5), 577−92.
(28) Wang, L.; Yang, L.; Yang, F.; Li, X.; Song, Y.; Wang, X.; Hu, X. Involvements of H_2O_2 and metallothionein in NO-mediated tomato tolerance to copper toxicity. *J. Plant Physiol.* **2010**, *167* (15), 1298−306.
(29) Zhang, A.; Zhang, J.; Ye, N.; Zhang, H.; Tan, M.; Jiang, M. Nitric oxide mediates brassinosteroid-induced ABA biosynthesis involved in oxidative stress tolerance in maize leaves. *Plant Cell Physiol.* **2011**, *52* (1), 181−92.
(30) Zhao, M. G.; Chen, L.; Zhang, L. L.; Zhang, W. H. Nitric reductase-dependent nitric oxide production is involved in cold acclimation and freezing tolerance in Arabidopsis. *Plant Physiol.* **2009**, *151* (2), 755−67.
(31) Schagger, H.; Von Jagow, G. Tricine-sodium dodecyl sulfate-polyacrylamide gel electrophoresis for the separation of proteins in the range from 1 to 100 kDa. *Anal. Biochem.* **1987**, *166* (2), 368−79.
(32) Rivero, R. M.; Shulaev, V.; Blumwald, E. Cytokinin-dependent photorespiration and the protection of photosynthesis during water deficit. *Plant Physiol.* **2009**, *150* (3), 1530−40.
(33) Miller, G.; Suzuki, N.; Ciftci-Yilmaz, S.; Mittler, R. Reactive oxygen species homeostasis and signalling during drought and salinity stresses. *Plant Cell Environ.* **2009**, *33* (4), 453−67.
(34) Xu, Y.; Gianfagna, T.; Huang, B. Proteomic changes associated with expression of a gene (ipt) controlling cytokinin synthesis for improving heat tolerance in a perennial grass species. *J. Exp. Bot.* **2010**, *61* (12), 3273−89.
(35) Mendel, R. R.; Hansch, R. Molybdoenzymes and molybdenum cofactor in plants. *J. Exp. Bot.* **2002**, *53* (375), 1689−98.
(36) Zarepour, M.; Kaspari, K.; Stagge, S.; Rethmeier, R.; Mendel, R. R.; Bittner, F. Xanthine dehydrogenase AtXDH1 from Arabidopsis thaliana is a potent producer of superoxide anions via its NADH oxidase activity. *Plant Mol. Biol.* **2010**, *72* (3), 301−10.
(37) Chevalier, C.; Bourgeois, E.; Just, D.; Raymond, P. Metabolic regulation of asparagine synthetase gene expression in maize (Zea mays L.) root tips. *Plant J.* **1996**, *9* (1), 1−11.
(38) Baum, G.; Lev-Yadun, S.; Fridmann, Y.; Arazi, T.; Katsnelson, H.; Zik, M.; Fromm, H. Calmodulin binding to glutamate decarboxylase is required for regulation of glutamate and GABA metabolism and normal development in plants. *EMBO J.* **1996**, *15* (12), 2988−96.
(39) Day, A.; Neutelings, G.; Nolin, F.; Grec, S.; Habrant, A.; Crônier, D.; Maher, B.; Rolando, C.; David, H.; Chabbert, B. Caffeoyl coenzyme A O-methyltransferase down-regulation is associated with modifications in lignin and cell-wall architecture in flax secondary xylem. *Plant Physiol. Biochem.* **2009**, *47* (1), 9−19.
(40) Shimizu, Y.; Maeda, K.; Kato, M.; Shimomura, K. Co-expression of GbMYB1 and GbMYC1 induces anthocyanin accumulation in roots of cultured Gynura bicolor DC. plantlet on methyl jasmonate treatment. *Plant Physiol. Biochem.* **2010**, *49* (2), 159−67.
(41) Droux, M. Sulfur assimilation and the role of sulfur in plant metabolism: a survey. *Photosynth. Res* **2004**, *79* (3), 331−348.
(42) Ferreira, S.; HjernØ, K.; Larsen, M.; Wingsle, G.; Larsen, P.; Fey, S.; Roepstorff, P.; Pais, M. S. Proteome profiling of Populus euphratica Oliv. upon heat stress. *Ann. Bot.* **2006**, *98* (2), 361−77.

(43) Golldack, D.; Dietz, K. J. Salt-induced expression of the vacuolar H+-ATPase in the common ice plant is developmentally controlled and tissue specific. *Plant Physiol.* **2001**, *125* (4), 1643−54.
(44) Hamilton, C. A.; Good, A. G.; Taylor, G. J. Induction of vacuolar ATPase and mitochondrial ATP synthase by aluminum in an aluminum-resistant cultivar of wheat. *Plant Physiol.* **2001**, *125* (4), 2068−77.
(45) Majoul, T.; Bancel, E.; Triboi, E.; Ben Hamida, J.; Branlard, G. Proteomic analysis of the effect of heat stress on hexaploid wheat grain: Characterization of heat-responsive proteins from total endosperm. *Proteomics* **2004**, *4* (2), 505−13.
(46) Kim, K.; Portis, A. R. Temperature dependence of photosynthesis in Arabidopsis plants with modifications in Rubisco activase and membrane fluidity. *Plant Cell Physiol.* **2005**, *46* (3), 522−30.
(47) Salvucci, M. E.; Crafts-Brandner, S. J. Relationship between the heat tolerance of photosynthesis and the thermal stability of Rubisco activase in plants from contrasting thermal environments. *Plant Physiol* **2004**, *134* (4), 1460−70.
(48) Dixon, D. P.; Lapthorn, A.; Edwards, R. Plant glutathione transferases. *Genome Biol.* **2002**, *3* (3), 30004.1−10.
(49) Xu, C.; Huang, B. Root proteomic responses to heat stress in two Agrostis grass species contrasting in heat tolerance. *J. Exp. Bot.* **2008**, *59* (15), 4183−94.
(50) Mizutani, M.; Ohta, D. Diversification of P450 genes during land plant evolution. *Annu. Rev. Plant Biol.* **2010**, *61*, 291−315.
(51) Larkindale, J.; Vierling, E. Core genome responses involved in acclimation to high temperature. *Plant Physiol.* **2008**, *146* (2), 748−61.
(52) Cutler, S. R.; Rodriguez, P. L. Finkelstein, R. R.; Abrams, S. R. Abscisic acid: emergence of a core signaling network. *Annu. Rev. Plant Biol. 61*, 651-79.
(53) Pang, Q.; Chen, S.; Dai, S.; Chen, Y.; Wang, Y.; Yan, X. Comparative proteomics of salt tolerance in Arabidopsis thaliana and Thellungiella halophila. *J. Proteome Res.* **2010**, *9* (5), 2584−2599.
(54) Gammulla, C. G.; Pascovici, D.; Atwell, B. J.; Haynes, P. A. Differential metabolic response of cultured rice (Oryza sativa) cells exposed to high- and low-temperature stress. *Proteomics* **2010**, *10* (16), 3001−19.
(55) Demirevska, K.; Simova-Stoilova, L.; Vassileva, V.; Feller, U. Rubisco and some chaperone protein responses to water stress and rewatering at early seedling growth of drought sensitive and tolerant wheat varieties. *Plant Growth Regul.* **2008**, *56* (2), 97−106.
(56) Yamazaki, T.; Komuro, I.; Kudoh, S.; Zou, Y.; Shiojima, I.; Hiroi, Y.; Mizuno, T.; Maemura, K.; Kurihara, H.; Aikawa, R. Endothelin-1 is involved in mechanical stress-induced cardiomyocyte hypertrophy. *J. Biol. Biochem.* **1996**, *271* (6), 3221−8.
(57) Jiang, Y.; Yang, B.; Harris, N. S.; Deyholos, M. K. Comparative proteomic analysis of NaCl stress-responsive proteins in Arabidopsis roots. *J. Exp. Bot.* **2007**, *58* (13), 3591−607.
(58) Yamaguchi-Shinozaki, K.; Shinozaki, K. Organization of cis-acting regulatory elements in osmotic-and cold-stress-responsive promoters. *Trends Plant Sci.* **2005**, *10* (2), 88−94.
(59) Heim, M. A.; Jakoby, M.; Werber, M.; Martin, C.; Weisshaar, B.; Bailey, P. C. The basic helix-loop-helix transcription factor family in plants: a genome-wide study of protein structure and functional diversity. *Mol. Biol. Evol.* **2003**, *20* (5), 735−47.
(60) Momcilovic, I.; Ristic, Z. Expression of chloroplast protein synthesis elongation factor, EF-Tu, in two lines of maize with contrasting tolerance to heat stress during early stages of plant development. *J. Plant Physiol.* **2007**, *164* (1), 90−99.